Bulletin of the Seismological Society of America, Vol. 98, No. 1, pp. 495–503, February 2008, doi: 10.1785/0120070054

Short Note

The Potential for Earthquake Early Warning in Italy Using ElarmS

by Marco Olivieri, Richard M. Allen, and Gilead Wurman

Abstract The new Italian National Seismic Network (INSN) is a dense network of broadband stations deployed for monitoring Italian seismicity. The network consists of 250 stations with a typical station spacing of ~40 km. Earthquake early warning is the rapid detection of an event in progress, assessment of the hazard it poses, and transmission of a warning ahead of any significant ground motion. We explore the potential for using the INSN real-time network for the purpose of earthquake early warning. We run the ElarmS early warning methodology off-line using a data set of more than 200 events with magnitudes between 2.5 and 6.0. A scaling relation for magnitude determination from the dominant period of the first seconds of signal following the *P* onset is developed from the data set. The standard deviation in the magnitude estimates using this approach is 0.4 magnitude units, and all event magnitude estimates are within ±0.75 magnitude units of the true magnitude. Given the existing distribution of seismic stations it takes an average of 10 sec after event initiation before the *P* wave has been detected at four stations. If we require a detection at four stations before issuing the first alert, then the blind zone, within which no warning would be available, has a radius of ~37 km. The ElarmS methodology can provide a warning earlier than this but with a greater uncertainty. An assessment of past damaging earthquakes across Italy shows that applying ElarmS with the existing seismic network could provide warning to population centers in repeats of past events. For example, in a repeat of the 1980 Irpinia earthquake Naples could receive an ~15- sec warning. The variations in the size of the blind zone and warning times for different regions can be used as a guide to selecting strategic locations for future station deployments.

Introduction

The advancement of seismic networks and communications now makes earthquake early warning (EEW) a feasible product for the seismic monitoring community. However, developing the methodologies, infrastructure, and end-user expertise necessary for an operational warning system remains a significant challenge. Given that we are unlikely to have the capacity for predicting earthquakes in the foreseeable future, effort has been focused on exploring the possibility of predicting earthquake ground motion using just the *P* wave of the seismic signal. This approach, on which the early warning methodology relies, allows us to exploit the *S*–*P* differential travel time for issuing an alert prior to damaging ground shaking. While *S* waves travel at two-thirds of the velocity of *P* waves, they usually have a significantly larger amplitude of ground shaking. The warning time is therefore the time until the *S* wave arrives at a specific location and will increase with distance from the epicenter of a damaging earthquake. This warning time can be used to take action to prevent or reduce the effects of the ground shaking, for example, isolating hazardous chemical systems and machinery, slowing and stopping transportation systems including trains, and personal protection measures such as getting school children under desks.

To maximize the available warning time from EEW systems, a dense network of stations is required in the epicentral area in order to minimize the time delay before receiving information about the event occurrence. A relationship that provides an estimate of the size and hazard of the earthquake using as little data as possible, just a few seconds of data after the *P* onset, is then required. ElarmS, the earthquake early warning system developed by Allen and Kanamori (2003) for California, uses the dominant period of the first few seconds of the *P* wave as the observable that scales with local magnitude M_L. The methodology was developed to maximize the warning time in a region where the population is collocated with the earthquake source region.

Both moderate and large earthquakes have caused significant damage and fatalities in Italy in the past few decades.

Protecting people and infrastructure from the next earthquake has become an important social and economic issue, in addition to an important goal of the seismological community. The earthquake source region is distributed throughout the country, but so is the new Italian National Seismic Network (INSN). California and Italy share similarities as hazardous seismicity is distributed throughout the region, and a dense broadband network is in place. We therefore use the ElarmS methodology as the basis for a feasibility study to explore the capacity of EEW to rapidly determine the hypocentral parameters of earthquakes and measure the time delay for making such information available in Italy using the INSN. Here we present the results of our off-line evaluation of ElarmS in Italy in order to test its capability to perform as an EEW for the region.

Seismic Risk in Italy

In the past century seven earthquakes with magnitude greater than 6.0 caused much damage and thousands of casualties. In particular, the 1976 Friuli earthquake caused 965 casualties and left about 45,000 people homeless. The Irpinia earthquake that hit a vast area in southern Italy, including the city of Naples (Fig. 1), caused 2914 casualties and 10,000 injuries and left about 300,000 people homeless. These earthquakes damaged wide areas surrounding the epicenter, sometimes larger than 100 km in radius. The wide distribution of the damage is due to a combination of the geology resulting in low rate of seismic attenuation in the region and of the poor quality of the buildings with respect to their resistance to ground shaking. Furthermore, it is noteworthy that in the recent past damage also occurred for moderate size earthquakes with M_L between 5 and 6.

Italy is a densely populated country with small towns and villages widely distributed and many old buildings. It is not sufficient to tackle the seismic hazard posed by the existing building stock through reconstruction or retrofitting the existing buildings. Such an approach would be unaffordable from an economical point of view and inappropriate from an historical and cultural one. We therefore look for other approaches to mitigate the impact of earthquakes across the country. EEW systems have been under development for several decades, and operational systems are now implemented in Japan, Taiwan, Mexico, and Turkey (Nakamura, 1988; Nakamura and Tucker, 1988; Espinosa-Aranda *et al.*, 1995; Wu *et al.*, 1998; Wu and Teng, 2002; Erdik *et al.*, 2003; Boese *et al.*, 2004; Kamigaichi, 2004; Horiuchi *et al.*, 2005; Wu and Kanamori, 2005; Wu and Zhao, 2006). These systems provide seconds to tens of seconds warning prior to ground shaking.

The warning time available from an EEW system increases with the distance from the epicenter, while the ground shaking hazard decreases with distance. As shown by Allen and Kanamori (2003), ElarmS implemented in a region in which earthquakes are collocated with buildings and population may not provide a warning in the area closest to the epicenter because the ground shaking may have begun before the information is gathered. However, records from

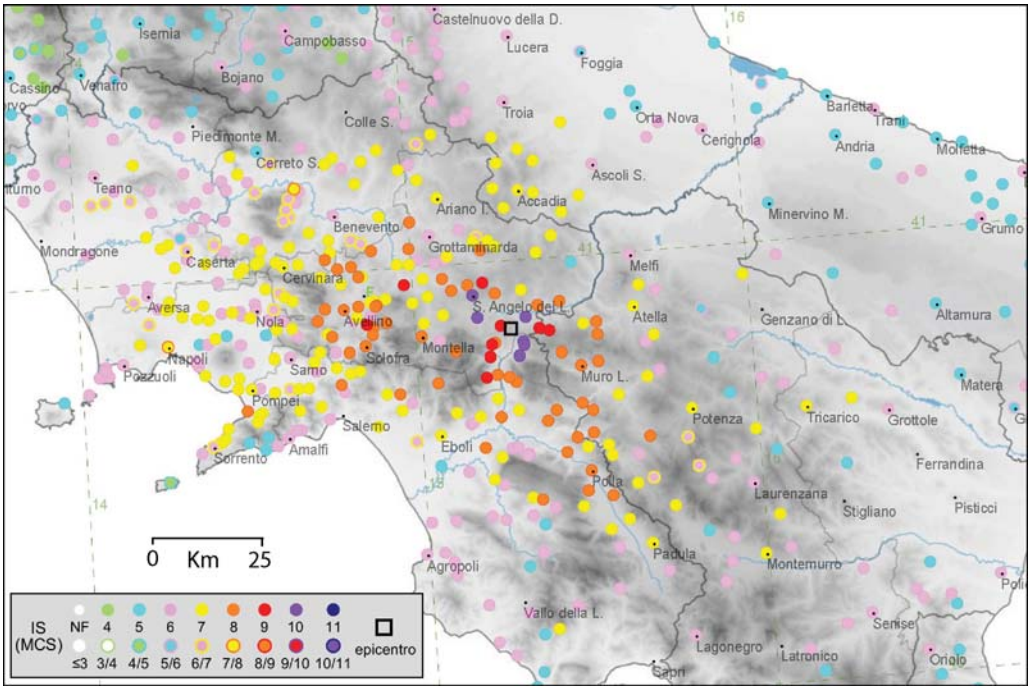

Figure 1. Distribution of observed intensities for the M_w 6.7 1980 Irpinia earthquake in southern Italy. The wide region affected by heavy damage is evident in terms of the seismic intensities of 7/8 and 8 measured more than 50 km from the epicenter. (Data are from Boschi *et al.*, 1997; figure provided by M. Locati).

the historical earthquake catalog (Boschi *et al.*, 1997) show the strong impact and damage over wide areas for earthquakes in Italy. This is illustrated in Figure 1, which shows the distribution of peak intensities for the 1980 M_w 6.7 Irpinia earthquake. While an EEW system may not be able to provide a warning in the epicentral region, warning would be available at greater distances. While the intensity will be lower at greater distances, the area affected is much greater. For this reason there is the potential to use an EEW system running over a dense network of seismic stations to mitigate the impact of the next destructive earthquake.

ElarmS Methodology

The magnitude of a local earthquake is usually determined by recording the whole waveform emanating from the event in order to estimate the maximum amplitude. This amplitude is corrected for epicentral distance, and the local magnitude, M_L, is determined. This approach requires one to a few minutes delay in order to obtain the necessary data from multiple stations. A reliable value for the magnitude requires averaging of individual station estimates. The delay is greater for strong earthquakes as *S*-wave amplitudes saturate at the closer stations, requiring data from more distant stations to be available.

ElarmS, described by Allen and Kanamori (2003), Allen (2004), and Wurman *et al.* (2007), succeeds in reducing this time limitation by coupling a simplified location technique with a magnitude estimate based on the dominant period (τ_p^{max}) and amplitude of the first 4 sec of the *P* wave, that is, the first arriving energy at the surface of the earth. The methodology uses two computational systems: the first one processes each single waveform in real time and delivers *P*-arrival picks. For each picked arrival on a vertical channel, it computes the associated dominant period and the peak amplitude for the next 4 sec. The second system gathers the information available from all stations every second, identifies earthquakes, and determines or updates the location and magnitude. With a dense network around the focal area, ElarmS can provide the first location estimate within 1 sec of the first station to trigger and provides the first magnitude estimate 1 sec later.

One of the two approaches to magnitude determination is the use of the dominant period, τ_p^{max}. τ_p^{max} is computed for each triggered vertical channel within 100 km. While single observations of τ_p^{max} show wide scattering, magnitude estimates tend to be stable and reliable when averaged over at least four stations (Lockman and Allen, 2007). Observations for Southern California (Allen and Kanamori, 2003), Northern California (Wurman *et al.*, 2007), and from a global data set (Olson and Allen, 2005) indicate that the dominant period scales with magnitude over a wide range of magnitudes (*M* 3.0–8.3). Olson and Allen (2005, 2006) discuss the possibility and the reliability of this kind of deterministic behavior of the rupture propagation which, for large earthquakes, can last more than the time interval used for measuring τ_p^{max}. The second approach to magnitude determination makes use of the amplitude of the *P* wave. Both the *P*-wave displacement and velocity are used using a method developed by Wu and Kanamori (2005). The magnitude estimated from these two approaches are averaged to provide the final ElarmS magnitude estimate (Wurman *et al.*, 2007).

Magnitude estimates are coupled with a simplified location schema that works best when there is a dense network in the epicentral area. As the first pick is available, the hypocenter is located at 8-km beneath the station. Once a second pick becomes available, the epicenter is moved to a location between the two based on the relative arrival times. Then, when three or more picks are available, grid searches for the best-fitting solution are used. The final output of ElarmS is a map of the distribution of the predicted ground shaking. The predicted ground shaking is estimated using the earthquake location, magnitude, and any available estimates of peak ground shaking close to the epicenter. A complete description of the methodology is available in Wurman *et al.* (2007).

The 1-sec schema provides updated earthquake information as the ground motion radiates from the hypocenter. As time advances the associated errors decrease, and the area already affected by the ground shaking widens with the time squared. The decision of when to act in response to a warning will therefore be different for different users depending on their specific needs and risks (V. F. Grasso and R. M. Allen, unpublished manuscript, 2007).

The off-line version of ElarmS as been developed to emulate a real-time data flow with the aim of exploring ElarmS performance during a range of events. This is a necessary step before planning a real-time implementation of EEW. Here we use the off-line version to determine region specific scaling relations and to assess the overall performance of ElarmS when applied to Italy.

Data Availability

In 2000 the INSN started a migration from a sparse short-period network to a dense broadband network. At present the INSN consists of about 250 stations to monitor a country of $300,000$ km^2 (Fig. 2). The network relies on a variety of digitizers and sensors and is continuously evolving. At present 120 stations are equipped with 40-sec velocity sensors (Trillium 40 s or Guralp CMG-40), and 23 stations have Lennartz 5-sec sensors; all are equipped with 24-bit digitizers. The MedNet Network (Mazza *et al.*, 2005) contributes to the INSN with 14 very broadband stations (STS-1 and STS-2 sensors) deployed in Italy. Some of the sites also have an accelerometer, but because these data are not transmitted in real time, we do not use them in this study. The data streams are telemetered to Rome via various telemetry systems including satellite connections, dedicated leased telephone lines, and the public administration network.

Olivieri and Schweitzer (2007) used a historical data set consisting of mostly a single waveform for each earthquake

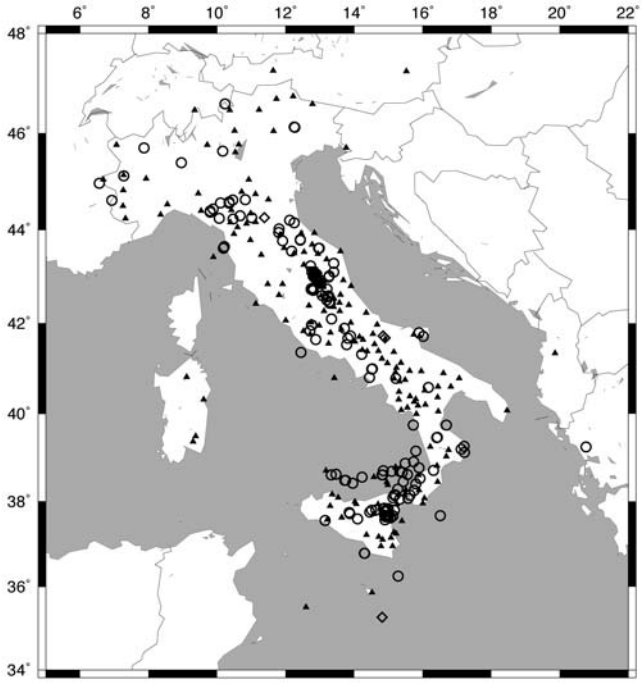

Figure 2. Map showing the distribution of INSN seismic stations (triangles) and the locations of the events used in this work (circles).

to show the existence of a linear relation between the log of the dominant period of the first few seconds after the *P* onset and the local magnitude M_L. The results were promising but also confirmed the observation by Allen and Kanamori (2003) that reliable estimates of the magnitude require averaging over several stations in order to reduce the scatter and minimize the error in the magnitude estimate. The new seismic network allows us to run a full test of ElarmS on the seismicity of Italy monitored by the INSN.

Since April 2006, we have been running ElarmS off-line to evaluate the capability of the network to provide data needed by ElarmS for producing location and magnitude estimates. Ten minutes after an earthquake occurs we emulate the synchronized real-time data flow and process all the waveforms for stations within 100 km of the epicenter. The system produces picks, dominant periods, and amplitudes from individual waveforms and uses them to determine location and magnitude providing an updated estimate of the ground-motion hazard every second. In addition to analyzing all events with $M \geq 2.5$ occurring since April 2006, we selected all past events in our database with magnitudes greater than 2.4 recorded by at least four broadband stations within 100 km of the epicenter. We also included some aftershocks of the 1997 Umbria earthquake (Amato *et al.*, 1998) recorded by a temporarily deployed network. Finally, 10 broadband records from single stations for large events are included to increase the magnitude range of the data set. They were recorded for events with magnitudes between M_L 5.0 and 6.0. The combined data set consists of 225 events with magnitudes between 2.5 and 6.0, and it is representative of the known seismicity in Italy.

Data Analysis

The earthquake hypocentral depths in California are small ranging from a few kilometers to ~15 km. For this reason the implementation of ElarmS in California does not estimate event depth; instead it is assigned to 8 km, the average depth. In Italy there is a much wider range of event depths that must be accounted for. A substantial number of subcrustal and deeper earthquakes occur in southern Italy and in the Tyrrhenian Sea subduction zone. To account for this specific feature of the Italian data we determine not just the epicenter but also event depth. This is achieved within the location algorithm by searching a 3D grid for the optimal event location. The grid consists of layers of nodes every 5 km, down to 660 km. While an accurate estimate of the depth is not important for the magnitude determination (τ_p^{max} does not show a distance dependence), a well-constrained depth is crucial for an accurate ground-motion prediction and also improves the estimation of the warning time.

Figure 3 shows the accuracy in earthquake location and the delay until a location is available at three stages of the location procedure. The first stage is when the first detection occurs, the second stage is when we have four *P*-wave detections, and the final stage is computed with all the *P* phases of stations within 100 km. As expected, the location error decreases as the number of *P*-wave detections increases, but the increasing accuracy is at the cost of an increased delay. When the first four *P*-wave picks are used, almost 90% of the location errors are smaller than 10 km and about 50% are within 4 km. These locations are available within 20 sec for most events and within 10 sec for half of the events (Fig. 3). Ten seconds after the origin the *S* wavefront is ~37 km from the epicenter (for a 10-km deep hypocenter) and is at ~74 km 20 sec after the origin. Comparing the four-station stage with the final location estimates, we conclude that the improvement in location is small while the additional time delay is several seconds.

For the magnitude estimation we test the improvements to ElarmS introduced by Wurman *et al.* (2007). They introduce a signal-to-noise ratio (SNR) data selection criteria to remove data for which the long-period seismic noise dominates the signal even though a pick was detected. They also introduce a test for clipped waveforms and exclude them from the analysis and introduce a time check on the predicted *S*-wave arrival to prevent the contamination of the *P*-wave dominant period measurement with a lower frequency *S*-wave signal.

To obtain the magnitude-period scaling relation for Italy we select all the events with at least four τ_p^{max} estimates with SNR $\geq$ 200. Individual waveform observations of τ_p^{max} within 4 sec of the *P*-wave trigger are plotted against M_L in Figure 4 along with the event averages. Blue dots in Figure 4 are

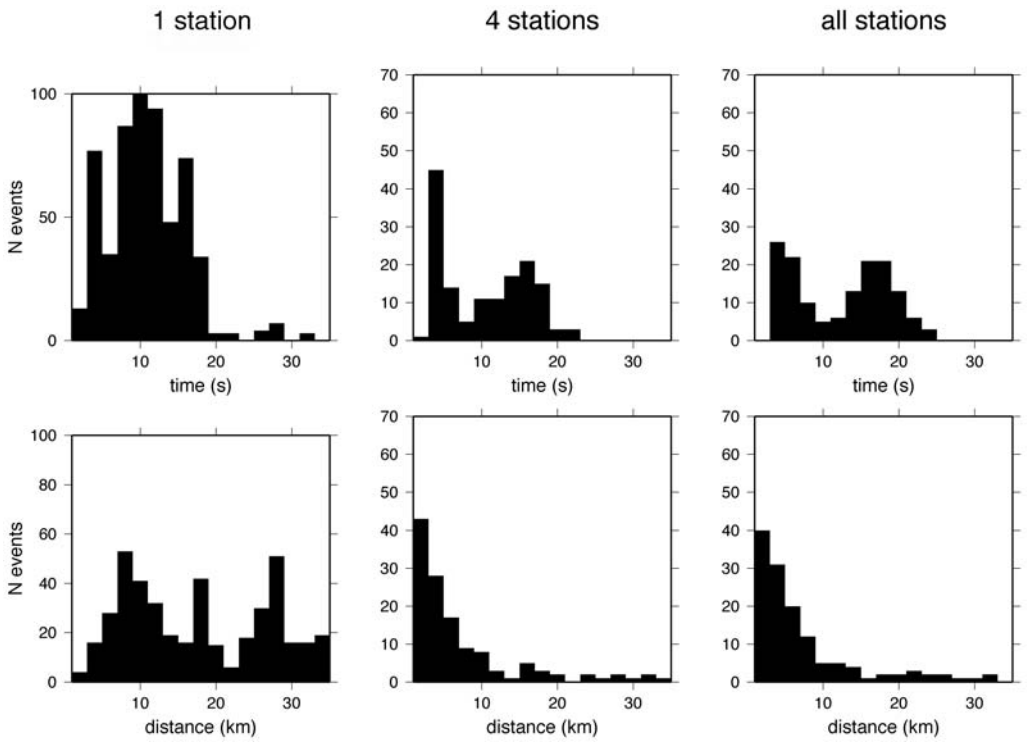

Figure 3. Results of the real-time location algorithm. The top row of histograms shows the time at which one-station, four-station, and all-station locations are available with respect to the earthquake origin time. The bottom row of histograms shows the corresponding location errors with respect to the manually reviewed locations provided by the INGV. Not surprisingly the locations improve significantly when four *P*-wave onset times are available compared to when only one is available. But the improvement with additional stations is marginal as shown by the difference between the four-station and all-station location errors.

the single station per event data included in the regression to expand the magnitude window. The linear regression of M_L on the logarithm of dominant period τ_p^{max} gives the best-fit relation

$$M_L = 3.05 \log(\tau_p^{max}) + 4.3 \quad (1)$$

with a standard deviation of 0.4 magnitude units. The best-fit relation is also plotted in Figure 4. To evaluate the utility of the observed magnitude versus the dominant period relation, we compare the ElarmS magnitude estimate with M_L determined by the network (Fig. 5). The total range of the errors in ElarmS magnitude estimates is 1.5 magnitude units, leading to a maximum error of ± 0.75 for all the events in our data set.

We also explored the use of *P*-wave peak ground displacement (PGD) and peak ground velocity (PGV) to provide an additional estimate of magnitude and potentially to reduce the error in the ElarmS magnitude estimate. Wurman *et al.* (2007) show that this approach can reduce the overall magnitude error in northern California. The approach has also been used in Taiwan (Wu and Kanamori, 2005) and Japan (Kamigaichi, 2004). Zollo *et al.* (2006) present evidence of a useful relation between the logarithm of PGD and magnitude using a data set from the whole Euro–Mediterranean region. However, we find that the variability in peak *P*-wave

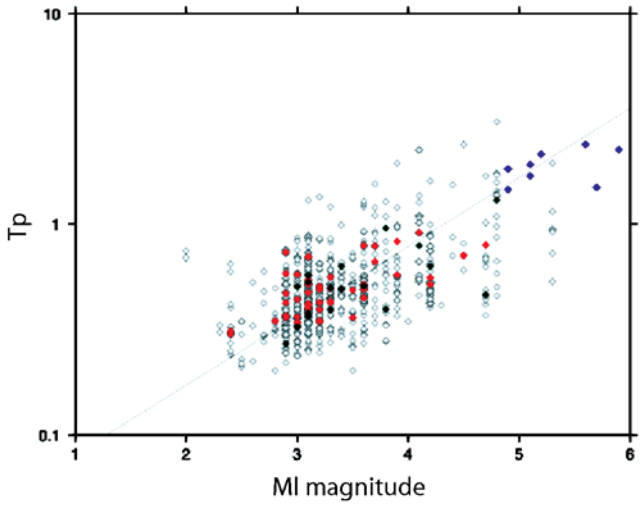

Figure 4. Dominant period, τ_p^{max}, versus magnitude. Single station observations over a 4-sec time window for which the SNR exceeds 200, gray diamonds; the average values of τ_p^{max} for events with at least four observations with SNRs greater than 200, red diamonds; observations for events from which only one station observation is available, blue diamonds. These are older events when there were far fewer stations in Italy than today. The best-fit line to the data is shown.

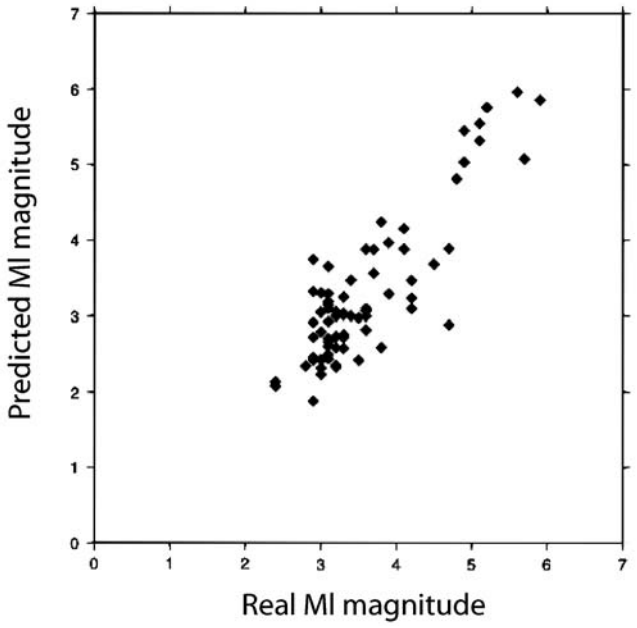

Figure 5. Comparison of the ElarmS predicted magnitude and network determined M_L. The ElarmS magnitude estimate is computed using equation (1). All event estimates fall within ±0.75 magnitude units of the M_L.

amplitude for different events with the same magnitude is comparable to the overall increase in the peak amplitude for the larger magnitude events in our data set. For this reason we concluded that we cannot use the PGD and PGV observables to improve our magnitude estimates in Italy.

Discussion

One of the limitations to an EEW system is the existence of a blind zone for each earthquake: a circular region around the epicenter within which no warning is available. The size of the blind zone is dependent on the time required to assess the hazard posed by an earthquake, which, in turn, is dependent on the proximity of seismic stations and the duration of *P*-wave data required at each station. We define an alarm time as being when four seismic stations have detected a *P* wave. While ElarmS provides the first hazard estimate based on just 1 sec of data from the first station to trigger, waiting for four stations to trigger provides a high degree of certainly in both the location and magnitude estimate. As shown in Figure 3, the elapsed time until four stations have detected *P*-wave arrivals is on average 10 sec and ranges from 2 to 24 sec for all the events we considered. These alarm time estimates translate into the radius of the blind zone. Alarm times of 2, 10, and 24 sec correspond to a blind zone radius of 7, 37, and 89 km, respectively, for a crustal earthquake. This is a limitation to the effectiveness of EEW. However, the size of the blind zone can be reduced by increasing the number of seismic stations across the country, and the Istituto Nazionale di Geofisica e Vulcanologia (INGV) is already planning to deploy at least 50 additional broadband stations in the near future to fill the gaps in the station spacing. In addition to reducing the area of the blind zones, these stations will also increase the warning times.

To illustrate the application of ElarmS we consider the 22 August 2005 M_w 4.6 Anzio earthquake that occurred offshore about 40-km southwest of Rome. This earthquake was well felt in the southern part of the city of Rome and all along the coast. This is a challenging case for early warning because the epicenter is offshore and quite far from the closest station, ROM9, located at INGV in Rome. Figure 6 shows the estimated epicenter, magnitude, and ground shaking prediction at four points in time. The location of Rome is shown by the stationary circle in Figure 6a–d, which represents the freeway surrounding the city. Given the distance of the closest station to the epicenter, the first *P*-wave detection does not occur until 11 sec after the event origin time. At 12 sec, the first estimate of the magnitude is available, *M* 3.2. The epicenter at this time is placed beneath the station, ROM9 (Fig. 6a). Two seconds later the second station triggers, and the location is placed between the stations based on arrival times (Fig. 6b). The magnitude estimate improves, going from 3.2 to 3.5. One second later, 15 sec after the origin, the third station triggers and the epicenter moves much closer to the real one (Fig. 6c). The magnitude is now averaged over three stations and uses a longer time window of data from the first two stations providing an estimate of *M* 4.2. One second later a fourth station triggers, and the location moves to within 5 km of the true location; the magnitude estimate remains at *M* 4.2. This represents the alarm time, at which point the 0 sec warning time contour runs through the center of Rome (Fig. 6d). However, this warning time estimate is a conservative one, and as shown by the horizontal component seismogram from ROM9 (Fig. 6e), there is still 2 sec until the *S*-wave arrival, which represents the peak ground motion for this earthquake. Therefore, despite the absence of stations close to the epicenter for this event, a warning could be issued before the peak ground shaking reaches the largest part of the city. The presence of an additional one or two stations closer to the coast would add a few additional seconds to the warning time.

To assess the capabilities of ElarmS using the present INSN network, we measure the distance of the fourth closest station from every point in the country (Fig. 7). This distance can be translated into the size of the blind zone at our alarm time should an earthquake occur at each point. Almost all of the country has four stations within 100 km; the exceptions are the nonseismic regions of southern Apulia and Sardinia. Nevertheless only very small patches of the country show at least four stations with 20 or 40 km. When four stations are within 20 or 40 km, the size of the blind zone is 13 or 26 km, respectively.

We compare the station distribution to the locations of earthquakes occurring in the past century with magnitudes greater than 5.0 from the International Seismological Centre (ISC) (2001) catalog (dots and diamonds in Fig. 7). For a

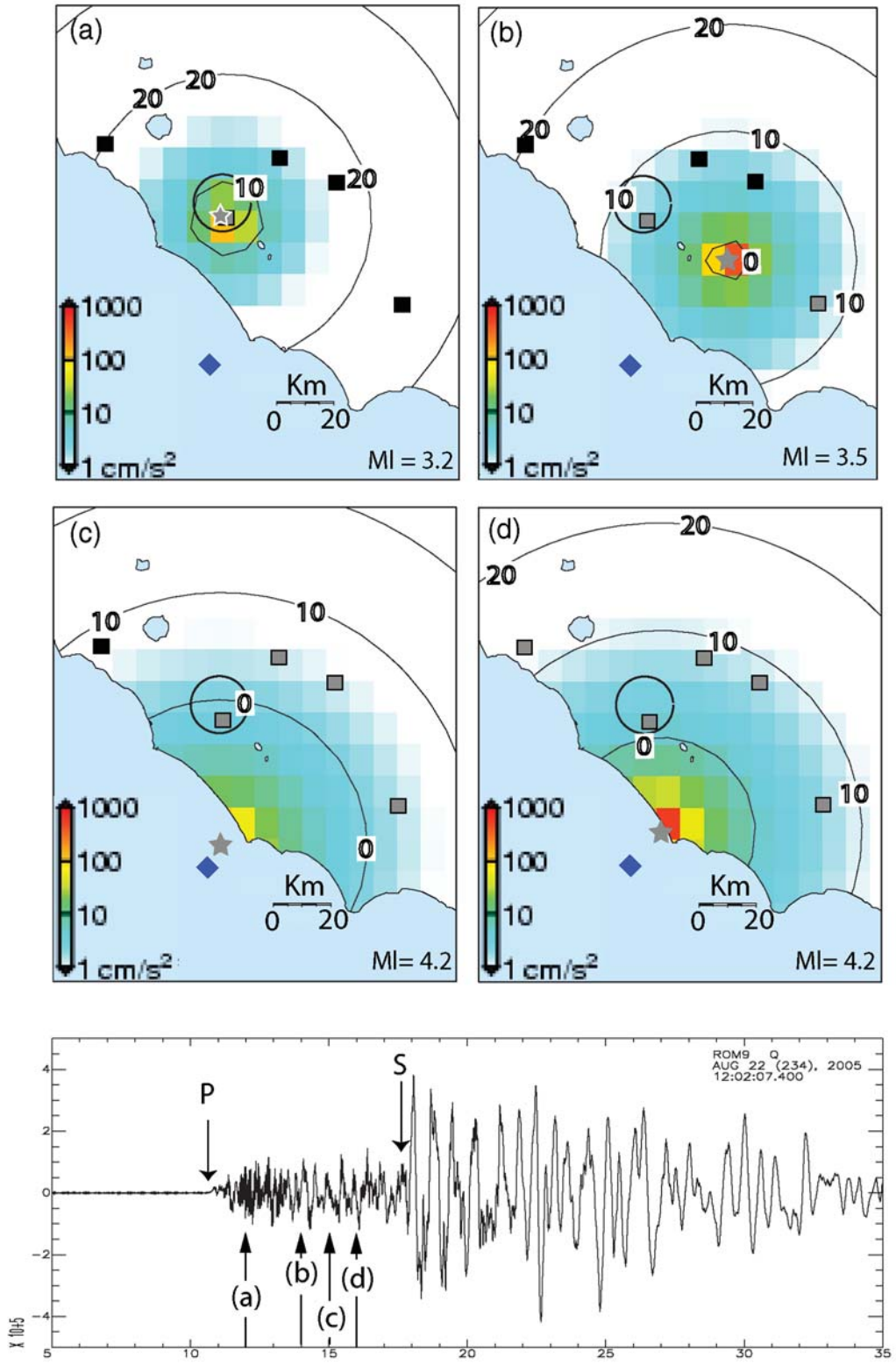

Figure 6. Example of the ElarmS processing and output for the 22 August 2005 M_w 4.6 Anzio earthquake near Rome. (a)–(d) Maps showing the predicted peak ground acceleration (color scale) at (a) 12 sec, (b) 14 sec, (c) 15 sec, and (d) 16 sec after the event origin time. The blue diamond is the true location, while the gray star is the ElarmS location estimate. The squares are the four closest stations and turn gray when they trigger on the *P*-wave arrival. The stationary circle represents the freeway circling Rome. Annotated circles show the warning time estimate as a function of time. (e) One of the horizontal component seismograms recorded at ROM9, close to the southeastern boundary of Rome. The *P*- and *S*-wave arrivals are annotated along with the times of the four hazard maps (a)–(d).

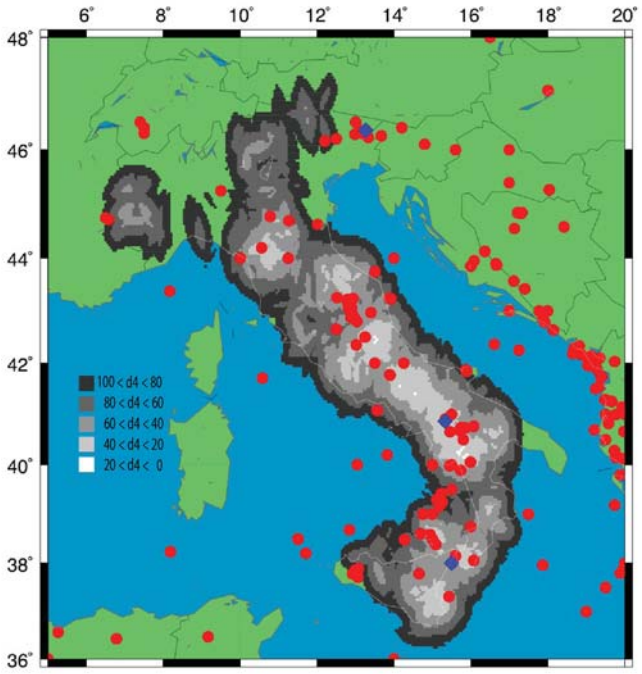

Figure 7. Map showing the density of INSN stations across Italy. The gray scale indicates the distance of the fourth closest station to all points in Italy. Black indicates that the fourth closest station is 80–100-km away; white indicates a distance of less than 20 km. Where there is no gray scale, there are not four stations within 100 km. Red dots are $M > 5.0$ earthquakes reported in the ISC (2001) catalog for the last century. The blue diamonds indicate three representative earthquakes discussed in the text: from north to south they are the 1976 Friuli, 1980 Irpinia, and 1908 Messina earthquake locations.

repeat of the 1980 Irpinia earthquake (the diamond at ~41° N) the size of the blind zone would be small, between 13 and 26 km, due to the dense network in the region. The city of Naples, which was widely damaged in 1980, would receive warning. In contrast, for a repeat of the Messina earthquake (the diamond at ~38° N) it would not be possible to provide warning to the two major towns that sit on the two sides of the Strait of Messina (Messina and Reggio Calabria). The blue diamond in the northernmost part of Italy represents the 1976 Friuli earthquake, and there are insufficient INSN stations in the region to provide early warning. However, a dedicated regional network run by the University of Udine and Istituto Nazionale di Oceanografia e di Geofisica Sperimentale (INOGS) monitors the region, and these stations could be used for early warning purposes.

The off-line tests presented do not tackle some important challenges to a real-time implementation. These include the processing of different waveforms that flow to the acquisition system with different latencies (the difference between the current time and the time of the last received sample) and the possibility of generating false alarms when processing continuous streams that include teleseisms and noise. However, since March 2006 ElarmS has been operating in a test mode as part of the real-time processing system in California. The ongoing tests will provide answers to many of the real-time operational questions.

Conclusions

Having tested the ElarmS methodology on a data set of 225 events in and around Italy, we find that the existing INSN could provide early warning using the ElarmS approach. Using the scaling relation we have developed here to estimate magnitude from the first four seconds of a vertical component seismogram after the *P*-wave onset, the standard deviation in the error of the predicted magnitude is 0.4 magnitude units, while the maximum error in this data set does not exceed ±0.75. This intrinsic uncertainty is similar to that observed for northern and southern California. It is also an acceptable uncertainty for EEW usage as we do not expect large differences in mitigating actions for earthquakes that differ by half a unit in magnitude.

While warnings would be possible for most of the country using the existing networks, the size of the blind zones is variable, ranging from ~13 km upwards depending on variations in the density of stations from region to region. Where dense station coverage exists, for example, the Irpinia region, the blind zone is small (13 to 26 km) and warning times are largest. For example, the city of Naples could receive ~15- sec warning in a repeat of the 1980 Irpinia earthquake. In regions with lower density, useful warnings are still possible as illustrated by the 2005 Anzio earthquake near Rome in which 1- or 2-sec warning could be provided to much of the city. The continuing growth of the INSN provides an opportunity to reduce the size of the blind zones and increase warning times by deploying stations in strategic sites in earthquake prone regions that also contain population concentrations. Figure 7 provides a guide that can be used to help determine the optimal locations for future seismic stations. The conversion of the INGV accelerometer network to real-time data transmission would also provide a significant improvement to the early warning capabilities. This would provide additional station sites and also provide a more robust mechanism for providing $\tau_p^{\max}$ observations in large events when there is a danger that high-gain velocity instruments may saturate before the 4 sec of *P*-wave data have been recorded.

Acknowledgments

This project was made possible through a collaboration between Istituto Nazionale di Geofisica e Vulcanologia (INGV), Rome, and the Berkeley Seismological Laboratory. Partial funding for Olivieri was provided by Italian Civil Protection Project Number DPC-S4. Funding for the development and testing of ElarmS was provided by the U.S. Geological Survey and the National Earthquake Hazard Reduction Program (NEHRP), Contract Number 06HQAG0147. Figures were produced using Generic Mapping Tools (GMT) by Wessel and Smith (1995). This work was done in the framework of the European Commission Project "Safer" (Contract Number 36935).

References

Allen, R. M. (2004). Rapid magnitude determination for earthquake early warning, in *The Many Facets of Seismic Risk*, M. Pecce, G. Manfredi and A. Zollo (Editors), Universita degli Studi di Napoli "Federico II", Napoli, 15–24.

Allen, R. M., and H. Kanamori (2003). The potential for early warning in southern California, *Science* **300,** 786–789.

Amato, A., R. Azzara, C. Chiarabba, G. B. Cimini, M. Cocco, M. Di Bona, L. Margheriti, S. Mazza, F. Mele, G. Selvaggi, A. Basili, E. Boschi, F. Courboulex, A. Deschamps, S. Gaffet, G. Bittarelli, L. Chiaraluce, D. Piccinini, and M. Ripepe (1998). The 1997 Umbria-Marche, Italy, earthquake sequence: a first look at the main shocks and aftershocks, *Geophys. Res. Lett.* **25,** no. 15, 2861–2864.

Boese, M., M. Erdik, and F. Wenzel (2004). Real-time prediction of ground motion from P-wave records (Abstract S21A-0251), *EOS Trans. AGU* **85,** (Fall Meet. Suppl.), S21A-0251.

Boschi, E., E. Guidoboni, G. Ferrari, G. Valensise, and P. Gasperini (1997). Catalogo dei Forti Terremoti in Italia dal 461 a.C. al 1990, ING e SGA Bologna, 644 pp (in Italian).

Erdik, M. O., Y. Fahjan, O. Ozel, H. Alcik, M. Aydin, and M. Gul (2003). Istanbul earthquake early warning and rapid response system (Abstract S42B-0153), *EOS Trans. AGU* **84,** (Fall Meet. Suppl.), S42B-0153.

Espinosa-Aranda, J. A., A. Jimenez, G. Ibarrola, F. Alcantar, A. Aguilar, M. Inostroza, and S. Maldonado (1995). Mexico City seismic alert system, *Seism. Res. Lett.* **66,** 42–53.

Horiuchi, S., H. Negishi, K. Abe, A. Kamimura, and Y. Fujinawa (2005). An automatic processing system for broadcasting earthquake alarms, *Bull. Seismol. Soc. Am.* **95,** 708–718.

International Seismological Centre (ISC) (2001), On-line Bulletin, http://www.isc.ac.uk (last accessed March 2007).

Kamigaichi, O. (2004). JMA earthquake early warning, *J. Jpn. Assoc. Earthq. Eng.* **4,** 1–4.

Lockman, A., and R. M. Allen (2007). Magnitude-period scaling relations for Japan and the Pacific Northwest: Implications for earthquake early warning, *Bull. Seismol. Soc. Am.* **97,** no. 1, 140–150, doi 10.1785/0120040091.

Mazza, S., M. Olivieri, A. M. Mandiello, and P. Casale (2005). The MedNet Network, in *Proc. of the Disaster Forecast and Prevention—Earthquake Monitoring and Seismic Hazard Mitigation in Balkan Countries Workshop*.

Nakamura, Y. (1988). On the urgent earthquake detection and alarm system (UrEDAS), in *Proc. 9th World Conf. Earthquake Eng. VII*, 673–678.

Nakamura, Y., and B. E. Tucker (1988). Earthquake warning system for Japan Railways' Bullet Trains: implications for disaster prevention in California, *Earthq. Volcanoes* **20,** 140–155.

Olivieri, M., and J. Schweitzer (2007). An empirical procedure for rapid magnitude estimate in Italy, *Bull. Seismol. Soc. Am.* **97,** no. 5, 1750–1755, doi 10.1785/0120060261.

Olson, E. L., and R. M. Allen (2005). The deterministic nature of earthquake rupture, *Nature* **438,** 212–215, doi 10.1038/nature04214.

Olson, E. L., and R. M. Allen (2006). Is earthquake rupture deterministic? (Reply), *Nature* **442,** E6.

Wessel, P., and W. H. F. Smith (1995). New version of the generic mapping tools released, *EOS* **76,** 329.

Wu, Y. M., and H. Kanamori (2005). Rapid assessment of damage potential of earthquakes in Taiwan from the beginning of P waves, *Bull. Seismol. Soc. Am.* **95,** 1181–1185.

Wu, Y. M., and T. L. Teng (2002). A virtual subnetwork approach to earthquake early warning, *Bull. Seismol. Soc. Am.* **92,** 2008–2018.

Wu, Y. M., and L. Zhao (2006). Magnitude estimation using the first three seconds P-wave amplitude in earthquake early warning, *Geophys. Res. Lett.* **33,** L16312.

Wu, Y. M., T. C. Shin, and Y. B. Tsai (1998). Quick and reliable determination of magnitude for seismic early warning, *Bull. Seismol. Soc. Am.* **88,** 1254–1259.

Wurman, G., R. M. Allen, and P. Lombard (2007). Toward earthquake early warning in northern California, *J. Geophys. Res.* **112,** B08311, doi 10.1029/2006JB004830.

Zollo, A., M. Lancieri, and S. Nielsen (2006). Earthquake magnitude estimation from peak amplitudes of very early seismic signals on strong motion records, *Geophys. Res. Lett.* **33,** L23312, doi 10.1029/2006GL0297795.

Istituto Nazionale di Geofisica e Vulcanologia
Roma, Italy
olivieri@ingv.it
(M.O.)

Department of Earth and Planetary Science
University of California, Berkeley
Berkeley, California 94720
(R.M.A., G.W.)

Manuscript received 12 March 2007